Multi-Cell Array of Nanogap Electrodes for Label-free Detection of Biomolecules

Musafargani Sikkandhar*
Institute of Microelectronics,
A*STAR (Agency for Science, Technology and Research)
Singapore
sikkandharm@ime.a-star.edu.sg

Yu CHEN
Institute of Microelectronics,
A*STAR (Agency for Science, Technology and Research)
Singapore
ORCID: 0000-0002-2149-667X

Ming-Yuan Cheng*
Institute of Microelectronics,
A*STAR (Agency for Science, Technology and Research)
Singapore
chengmyn@gmail.com

***Abstract* — Impedimetric biosensors are predominantly used for *in vitro* device applications due to their portability. However, these devices suffer from thermal noise due to electric double layer (EDL) at low frequencies (<100 KHz). Hence, we disclosed a novel multi-cell nanogap electrode array with nanogap size (~100 nm) electrode to reduce this parasitic noise from EDL. Thus, it increased the sensitivity of detection of interested biomolecules. The proposed electrodes are fabricated on the SiO_2 substrate using Aluminum (Al) electrodes with the passivation of Hafnium oxide (HfO_2) on it. We evaluated the fabricated electrodes in potassium chloride (KCl) solution to determine the sensitivity of the sensor with decreasing of the gap between the electrodes. Hence, the electrode with the smallest gap size (~100 nm) is evaluated for the determination of hybridization of TNF-α protein to demonstrate the biomedical application of the developed sensor.**

Keywords* — *nanogap, sensor, biosensor, electric double layer, protein

I. Introduction

Impedimetric biosensors are emerging as a breakthrough technology for early detection of biomarkers of fatal diseases [1]. These biosensors have been established as a replacement for the conventional enzyme-linked immunosorbent assay (ELISA) due to its low cost, ease of operation and rapid response time. Multiple approaches of biosensors such as optical and electrochemical-based techniques are developed. However, electrochemical techniques are cheaper as it is devoid of expensive light source for detection.

Electrochemical biosensors with geometry from planar to circular are fabricated to improve the sensitivity of detection of the target biomolecules [2]. However, each of the proposed ideas possesses its own manufacturing complexity. Planar interdigitated electrodes (IDEs) have been extensively used for biomolecular detection applications [3]. The geometry of the IDEs is critical for the sensitivity of detection. *Van Gerwan et al*. [4], studied that the planar IDEs with reduced gap and width will have better sensitivity due to the shortcoming of electronic thermal noise arising from the electric double layer (EDL) as shown in Fig. 1. Hence, it masks the critical information of

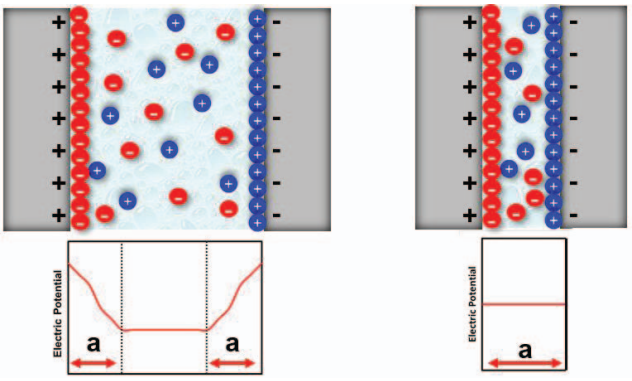

(a) (b)

Fig. 1 Electric potential as a function of distance between electrodes of (a) large gap and (b) nanogap

biomolecules of interest for detection and reduces the resolution. To overcome this, we disclosed a novel multi-cell nanogap electrode array to reduce the impedance of the EDL by reducing the gap between the electrodes smaller than the thickness of the EDL (typical thickness is around 100 nm) [5]. Innovatively, we developed a three-dimensional nanogap electrode with a depth of 600 nm to increase the sensitivity of detection. These nanogap interdigitated electrodes (nIDEs) possess versatile application such as single molecule recognition, nucleic acid lysing and identification, chemical kinetics study, plasmonic sensor and laser source development (Fig. 2).

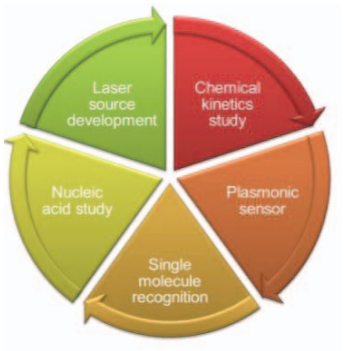

Fig. 2. Versatile applications of nIDEs

*The authors contributed equally to the work as corresponding authors.

In this paper, we simulated the nanogap electrode array of various gap sizes and electrode thickness as using COMSOL Multiphysics® software to study the resultant electric potential energy distribution. Each electrode array is connected in series to form a multi-cell array of nanogap electrode. Usually, gold (Au) electrodes are used for biomedical applications due to its biocompatibility nature. However, developing nanogap high aspect ratio structures requires plasma etching which is not possible with gold. Also, using the wet chemical etching results in under etching and uniformity issues. The proposed idea is evaluated by fabricating the Aluminum (Al) electrodes. We deposited 30 nm thickness of Hafnium oxide (HfO_2) using atomic layer deposition (ALD) technique to further reduce the gap between the electrodes due to its biocompatibility and high dielectric constant [6]. The gap size and thickness of the fabricated nanogap electrodes are validated using focused ion beam scanning (FIB) and defect review - scanning electron microscope critical dimension (DR-SEM CD). We demonstrated the fabricated electrodes to determine the hybridization of biotin with streptavidin aptamers.

II. Design and Fabrication

A. Electrode Design Simulation

We simulated the design of the array of nanogap electrodes with the finite element analysis method using the COMSOL Multiphysics® software. The nanogap electrode of interdigitated comb structure is designed with the different gap sizes of 200, 400, 600 nm and 1 µm and thickness of 200, 400 and 600 nm. We studied the performance of the electric potential by tuning the depth of the electrode at from 200 to 600 nm. The metal layer of the electrode chosen is Al, while the dielectric material used for the simulation is water. The permittivity of the Al and water is set to be 1 and 80 respectively. We applied the voltages of 1V and 0V on the electrode and studied electric potential energy distribution between the electrodes.

B. Electrode Mask Preparation

In this study, we used the negative photoresist to pattern the array of nIDEs as shown in Fig. 3. During the patterning of structures, we included dummy structures towards the end of the array. The purpose of these dummy structures is to reduce the non-uniformity of etching on the start and end of the fingers of nIDEs.

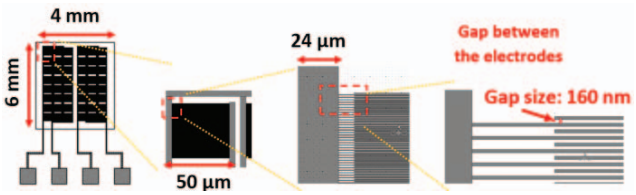

Fig. 3. Electrode design and layout development

C. Electrode Fabrication

The fabrication process flow is summarized in Fig. 3. An 8" silicon wafer is deposited with silicon dioxide (SiO2) of 1 µm depth followed by 30 nm of Chromium (Cr) for adhesion. A thick layer of Al (consists of 5% copper (Cu)) of thickness 600 nm is deposited on the adhesive layer to form the electrode. Using reactive ion etching (RIE) with BCl_3/Cl_2, the determined gaps between the electrodes are achieved by etching the Al electrode along with the layer of Cr. On the resultant Al electrode structure, we deposited 30 nm thickness of HfO_2 using ALD technique to further reduce the gap between the electrodes. Preferably, HfO_2 was selected over the other oxides due to its high dielectric constant (16.64). The gap size and thickness of the fabricated nanogap electrodes are validated using FIB and DR-SEM CD. The complete fabrication process flow is shown in Fig. 4.

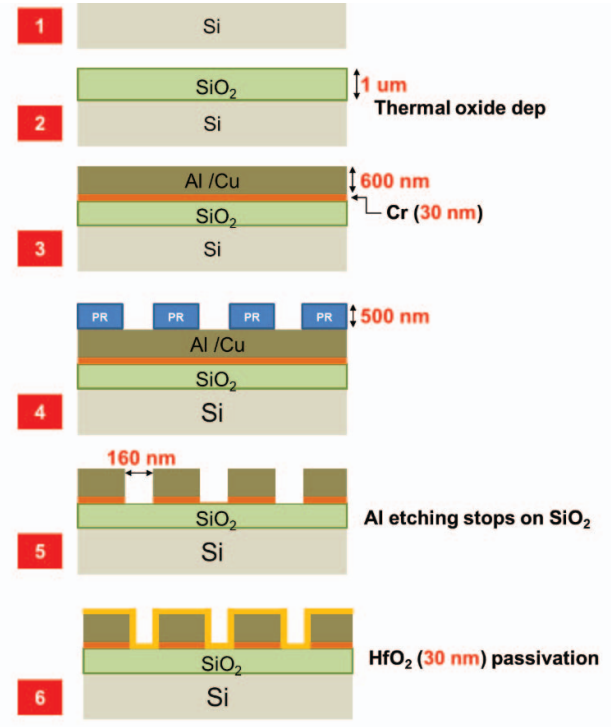

Fig. 4. Fabrication process flow

D. Wafer Dicing and Chip Preparation

The fabricated wafers are diced out using laser source and diced out chips are cleaned in acetone, iso-propyl alcohol (IPA) and distilled water (DIW) using sonicator for 3 minutes of each of the chemicals. The cleaned chips are dried using nitrogen (N_2) gas. The dried chips are cleaned using plasma source for 5 minutes. The chips are eventually wire bonded on to the printed circuit board (PCB) as shown in Fig. 5.

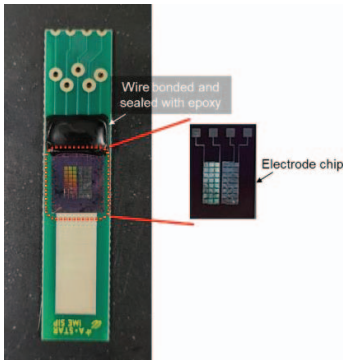

Fig. 5. Fabricated electrode chip wire bonded on PCB

III. Materials and Methods

A. Chemicals and Reagents

We purchased the following chemicals from Sigma Alderich, potassium ionophore, (3-Aminopropyl) tri ethoxy silane (APTES), 2-Iminothiolane hydrochloride, 1-Ethyl-3-(3 dimethyl aminopropyl) carbodiimide (EDC), N-hydroxy succinimide (NHS), 4-Aminothiophenol (4-ATP), 2-naphthalenethiol (2-NT), recombinant human TNF-α protein (TNF-α), Anti-TNF-α antibody (Anti-TNF-α), ethanol, bovine serum albumin (BSA) and phosphate buffered solution (PBS).

B. Potassium ionophore coating and characterization

The potassium ionophores of 12 µL is casted on the electrodes and stored under the vacuum for 12 hours. Later, the chip is conditioned in 1 mM potassium chloride (KCl) solution for 12 hours. This conditioning technique improves the continuous movement of ions across the membrane. The conditioned chips are validated in various concentrations of KCl solutions ranging from 0.01 – 1 mM using the Autolab software to read the impedance spectrum at 1 mV (frequency range of 20 Hz – 3KHz). Also, we measured the resistance of KCl solution at its various concentrations [7].

C. Hybidization of protein

10 µg/mL of TNF-α protein is dissolved in 14 mM Traut's reagent to form a thiolated solution. The thiolated solution is coated on the fabricated electrodes for testing. Meanwhile, 0.4 mL of 50 mM EDC is mixed with 0.1 mL of 1 mg/mL anti-TNF-α solution and incubated for 5 min. Subsequently, 0.1 mL of NHS is dissolved in the mixture and incubated for 5 min. EDC-NHS anti-TNF-α solution is modified with 4-ATP and incubated for 30 mins. The mixture is coated on the electrode (gap of 100 nm CD) after incubating with the BSA to bind with the specific sites of the thiolated protein [8].

D. Electro-Impedance Spectroscopy

The chips with proteins immobilized on it of various concentrations are tested using the Autolab software at 1 mV (frequency range of 20 Hz- 3KHz). The chips are validated in both dry and wet phase. During dry phase, air is used as medium of contact with the immobilized proteins, while the chips are dipped in PBS solution for wet phase.

IV. Results and Discussion

A. Electrode Design Simulation

Based on the study of simulated design structures, we studied the electric potential energy distribution by tuning the gap (G), thickness (T) and depth (D) of the electrode. It was understood that by narrowing the gap between the electrodes improved the resultant electric potential energy to be higher than larger gaps (Fig.6). The thickness of the electrode did not produce significant impact as tuning the gap between the electrodes. With increased thickness of the electrode, electric potential energy increased only by 0.002 fJ/nm as shown in Fig. 7. However, we observed that increasing the depth of the electrode produced significant improvement of electric potential at a rate of 0.0125 fJ/nm as shown in Fig. 8. Hence, the electrodes with the smallest gap and largest depth produces significant electric potential energy.

B. Electrode Fabrication

Based on the simulation results, we understood the electrodes with smallest gap and largest depth provides significant results. We successfully achieved the gap of interdigitated electrodes to be ~100 nm, ~300 nm and ~500 nm (after HfO_2 coating) and thickness of 200 nm and 400 nm with repeatable results. The smallest of the nanogap between the electrodes that we achieved is ~96 nm. Based on the DR-SEM results, we able to review the SEM CD of the gap before depositing the HfO_2. The thickness of the HfO_2 achieved is 30 ± 6 nm. Also, we have shown the FIB (Fig. 9) and DR-SEM CD (Fig. 10) data to support the fabrication of the device achievements. The triangle structure in the FIB image (Fig. 9) is not a special structure, however, due to the angle of tilting and non-uniform bottom surface.

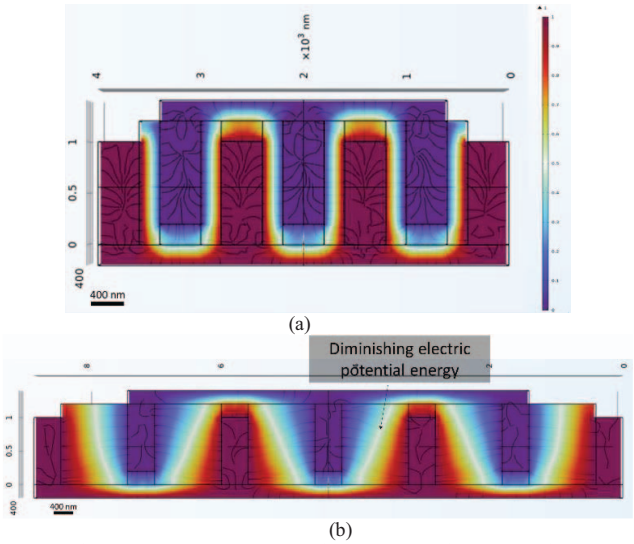

Fig. 6. Electric potential energy distribution across the simulated electrode structure of thickness with a gap of (a) 200 nm and (b) 1 µm. We understood the electric potential energy diminished with increased gap between the electrodes

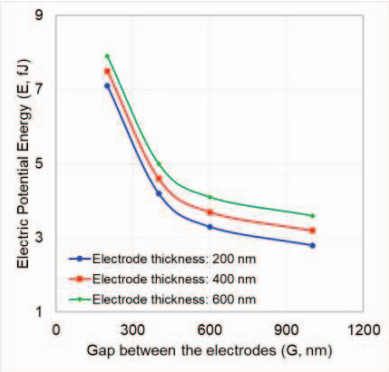

Fig. 7. Simulation results of electric potential energy distribution with various gaps and thickness of the electrode

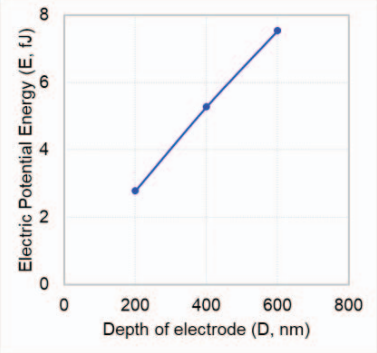

Fig. 8. Simulation results of electric potential energy distribution with various depth of the electrode

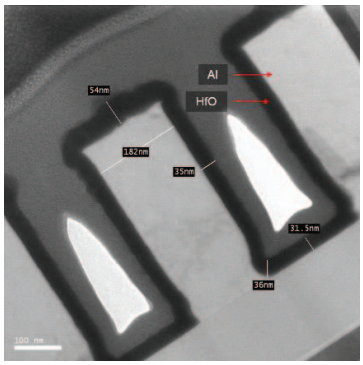

Fig. 9. Cross section of nanogap interdigitated electrodes

C. *Electro-impedance spectroscopy*

The chips coated with potassium ionophore displayed the impedance spectroscopy at various concentrations of KCl is as shown. in Fig. 11. Also, we plotted the resistance of the KCl solution in the same plot. The spectrum of impedance due to K+ varies from 80 KΩ to 10 KΩ. It is understood the sensitivity of change of impedance with the change of concentration of KCl is calculated to be 27 KΩ / decade of concentration. The minimum concentration of the KCl that can be measured with the developed device is 0.01 mM. Also, the resistance of the KCl solution varies in the MΩ range.

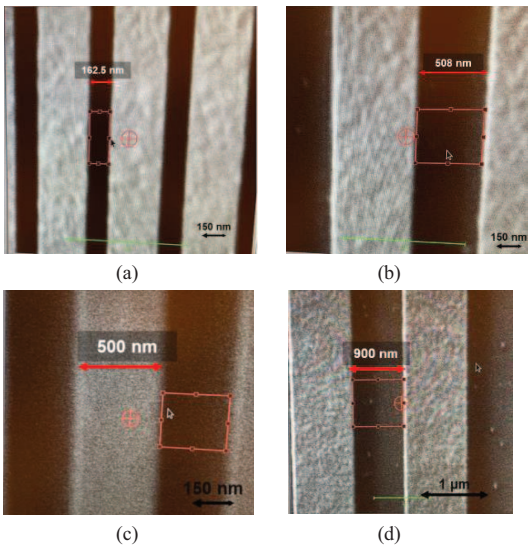

Fig. 10. DR SEM CD data collected to measure (a), (b), (d) gap between the electrodes and (c) thickness of the electrodes after the fabrication of Al electrodes without the HfO_2 deposition

The chips coated with various concentrations of TNF-α protein is studied under impedance spectroscopy at two different phases, namely, dry and wet phase. During the dry phase, we observed that the impedance decreased at a rate of 80-90 times for 100 times of increase in the concentration of protein binding at a frequency of 230 Hz (1 mV alternating current) as shown in Fig. 10. However, during the wet phase measurement, the sensitivity of detection drops significantly as shown in Fig. 11. It is suspected due to the washing away of proteins in PBS. The overall device operating impedance range is from 6 MΩ to 1 KΩ. The minimum concentration of the protein that can be detected using the developed device is 0.1 µM.

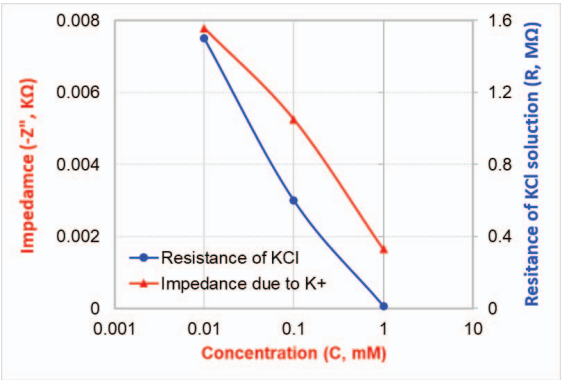

Fig. 11. Impedance spectrum due to K+ and resistance of KCl at various concentrations of KCl

V. Conclusion

In this work, we developed a multi-cell array of nanogap electrodes by tuning the dimensions of the electrode, namely, gap between the electrodes and its thickness. We achieved the following in this paper:

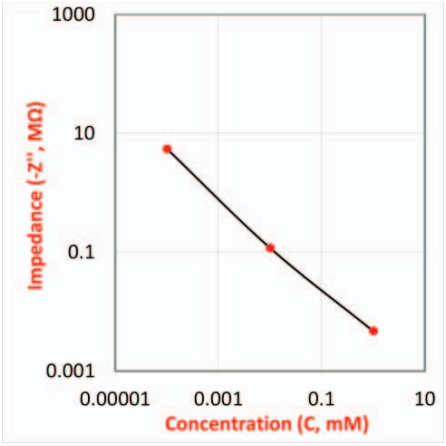

Fig. 12. Impedance spectrum for the various concentrations of TNF-α protein at 230 Hz in dry phase

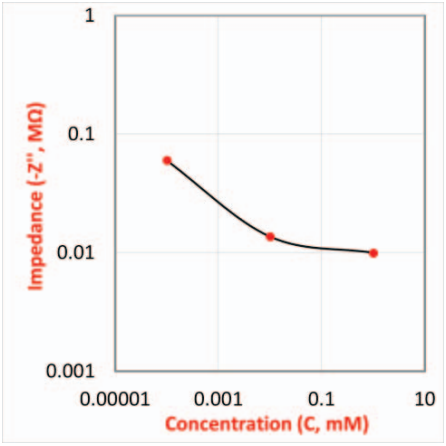

Fig. 13. Impedance spectrum for the various concentrations of TNF-α protein at 230 Hz in wet phase

VI. Conclusion

In this work, we developed a multi-cell array of nanogap electrodes by tuning the dimensions of the electrode, namely, gap between the electrodes and its thickness. We achieved the following in this paper:

1. We simulated a nanogap interdigitated electrodes of different design parameters using COMSOL Multiphysics® software to study the electric potential energy distribution between the electrodes.
2. Based on the DR-SEM and FIB results, we have successfully demonstrated the fabrication of electrodes with the gap size of 100 nm, 300 nm, and 500 nm and thickness of 200 nm and 400 nm.
3. Using Autolab impedance spectroscopy, it was observed that electrodes with gap size of ~100 nm, thickness of 200 nm and depth of 600 nm at 230 Hz frequency in KCl solution has a sensitivity of 27 KΩ / decade. Hence, smaller gap and larger depth of the electrode aids to improve the sensitivity of the sensor.
4. We observed that the fabricated chip exhibited drop in impedance by 80-90 times for 100 times of increase in the concentration of TNF-α protein binding at a frequency of 230 Hz.
5. The minimum detection of TNF-α protein concentration of our developed sensor is 0.1 µM.

The developed biosensor has the potential to be used for label free detection of biomarkers for fatal diseases at homecare. Thus, it simplifies the laboratory procedure into an on-chip process technology for rapid testing and reduces the amount of sample collected for testing. In our future work, we are evaluating on the single chip multiplexing such than > 10 biomolecules are detected using the single chip. Hence, these nanogap electrode arrays are potentially to be used *in vitro* device (IVD) applications at low frequency alternating current with minimal noise generated.

Acknowledgement

We would like to thank **Norhanani Binte Jaafar** and **Dr J. Perumal** for supporting the wire bonding and biological work respectively.

References

[1] M. Nemati, M.A. Farajzadeh, M.R. Afshar Mogaddam, and A. Pourali, "Recent Advances in Impedimetric Biosensors Focusing on Myocardial Infarction Diagnosis," Critical Reviews in Analytical Chemistry, pp. 1-14, 2022.

[2] H.J. Sheen, B. Panigrahi, T.R. Kuo, W.C. Hsu, P.S. Chung, Q.Z. Xie, and Y.J. Fan, "Electrochemical biosensor with electrokinetics-assisted molecular trapping for enhancing C-reactive protein detection," Biosensors and Bioelectronics, vol. 210, pp. 114338, 2022.

[3] E. Kosri, F. Ibrahim, A. Thiha, and M. Madou, "Micro and Nano Interdigitated Electrode Array (IDEA)-Based MEMS/NEMS as Electrochemical Transducers: A Review," Nanomaterials, 12th ed., vol. 23, pp. 4171, 2022.

[4] P. Van Gerwen, W. Laureyn, A. Campitelli, P. Jacobs, P. Detemple, K. Baert, and R. Mertens, "Cost effective realization of nanoscaled interdigitated electrodes," Journal of Micromechanics and Microengineering, 10th ed., vol. 3, pp. N1, 2022.

[5] Z.G. Namhil, C. Kemp, E. Verrelli, A. Iles, N. Pamme, A.M. Adawi, and N.T. Kemp, "A label-free aptamer-based nanogap capacitive biosensor with greatly diminished electrode polarization effects," Physical Chemistry Chemical Physics, 21st ed., vol. 2, pp. 681-691, 2019.

[6] M. Peron, S. Cogo, M. Bjelland, A.B. Afif, A. Dadlani, E. Greggio, and J. Torgersen, "On the evaluation of ALD TiO2, ZrO2 and HfO2 coatings on corrosion and cytotoxicity performances," Journal of Magnesium and Alloys, 9th ed., vol. 5, pp. 1806-1819, 2021.

[7] M. Sikkandhar, Y. Chen, and C. Ming-Yuan, "Reference Free Ion-Selective Electrode for Sensing Potassium Ions," IEEE 23rd Electronics Packaging Technology Conference (EPTC), pp. 205-208, 2021.

[8] J. Perumal, H. Q. Lim, A.B. E. Attia, R. Raziq, D.I. Leavesley, Z. Upton and M. Olivo, "Novel cellulose fibre-based flexible plasmonic membrane for point-of-care SERS biomarker detection in chronic wound healing," International Journal of Nanomedicine, vol. 16, pp. 5869, 2021.